University of Medicine and Pharmacy "Carol Davila" Bucharest
Faculty of Medicine
Doctoral School

PhD Thesis

Maxillo-palatal anatomy studies

- SUMMARY -

Scientific leader
Prof.Univ.Dr.Habil. Mugurel Constantin Rusu

Doctorand
Dr.Andrei Valentin Iamandoiu

Bucharest, 2024

Contents of the PhD Thesis

Introduction

In the modern period, with the rapid spread of implant-prosthetic treatment, the importance of accurate data on the jaw and mandible has increased. The structural characteristics of the alveolar processes change significantly after tooth loss. The maxilla, formed by the two maxillary bones, has thinner cortical bone than the mandible and its structure is dominated by cancellous (trabecular) bone.

CT scans are ideal for assessing bone anatomy and allow accurate measurements useful, for example, for the analysis of the pterygopalatine fossa and the large palatine canal. Cone Beam Computed Tomography (CBCT) scans are used in dentistry.

The basic assumption of my research was that many pre-existing anatomical data in the literature cover a real range of anatomical variations reduced by comparison with the details provided by sectional anatomy in cone-beam computed tomography. For these reasons, the main aim of my PhD work was to identify anatomical possibilities, some subtle, at the level of the maxillary floor of the skull. These are of unquestionable clinical interest and can be assessed in cone-beam computed tomography on a case-by-case basis by the stomatologist.

1 Anatomo-imaging investigations of the large palatine foramen

1.1 Introduction

Looking at the large palatine canal (MPC) and its inferior opening, the large palatine foramen, previous studies have documented the following variables:

- GPM position relative to the maxillary molars or to various landmarks of the hard palate, such as the median plane, the posterior edge of the hard palate, the incisal foramen, the anterior nasal spine or the alveolar ridge;
- GPM position relative to the pterygoid hook, 10-16 mm antero-medial to it;
- bilateral topographic symmetry of the GPM;
- GPM diameter;
- CPM angulation;
- CPM length;
- GPM shape (e.g. oval, chain, slot, round);
- number of GPM (absent, single, double);

- CPM length and pterygopalatine fossa (PPF) height.

I have not been able to identify in the literature much consistent data, such as those from recent studies, on the bilateral geometric and morphometric symmetry, respectively, of CPM..

1.2 Material and method

Cone Beam CT (CBCT) scan records from 104 dental patients (43 male, 61 female,) were studied retrospectively. CBCT scanning was done for dental reasons with an iCat scanner (Imaging Sciences International, Hatfield, USA) (resolution 0.250, FOV 130^{o} , image matrix size 640 × 640). CBCT files were exported in *.dcm format and anatomically evaluated with Planmeca Romexis Viewer 3.5.0.R software, as in previous studies. Patients had informed consent to use anatomical information in the study, provided that files were anonymized and confidentiality was maintained.

We followed the topographic types of GPM referred to maxillary molars, noting "E" the presence of edentulousness in that site. We defined type 1 for GPM placed at the interproximal septum between the first two molars of the maxilla (M1/M2), type 2 for GPM medial to the second molar of the maxilla (M2), type 3 for GPM in line with the M2/M3 interproximal septum, type 4 for GPM in line with M3 and type 5 for GPM located distal to M3.

We used a secondary retrospective batch of 72 CBCT records to determine the variability of distances between the GPM and the incisive fossa and posterior nasal spine, respectively. There were 23 male and 49 female cases. In this study we defined types by value groups as follows:

1) for GPM-incisor fossa distance: type A = < 35 mm, type B = 35-40 mm, type C = 40-45 mm and type D = > 45 mm
2) for distance GPM-posterior nasal spine: type 1 = < 14 mm; type 2 = 14-15 mm; type 3 = 15-16 mm; type 4 = 16-17 mm; type 5 = 17-18 mm; type 6 = 18-19 mm; type 7 = 19-20 mm; type 8 = > 20 mm.

1.3 Results - Topography of the large palatine hole referred to the maxillary alveolar-dental arch

1.3.1 Results in the overall lot and grouped by gender

Of the 104 cases, 63 (60.5%) had terminal edentulousness of the jaw, 12 (11.5%) unilateral and 51 (49%) bilateral. Out of 43 male subjects, 4 (9.3%) had unilateral distal maxillary edentations, another 18 (41.8%) had bilateral terminal maxillary edentations. Of 61 female subjects, 8 (13.1%) had such unilateral edentations and 33 (54%) bilateral.

We did not identify in the investigated group the presence of GPM at the interproximal septum between M1 and M2.

	2+2	2+3	3+3	3+4	4+4	4+4E	4E+4E	5+5	5+5E	5E+5E
M	0	0	2	2	10	4	14	7	0	4
F	2	1	0	0	9	7	27	8	1	6
TOTAL	***2***	***1***	***2***	***2***	***19***	***11***	***41***	***15***	***1***	***10***

Tab. 1- 1 - Bilateral determinations of the position of the large palatine foramen in the study group (N=104), males (M, n1=43) and females (n2=61).

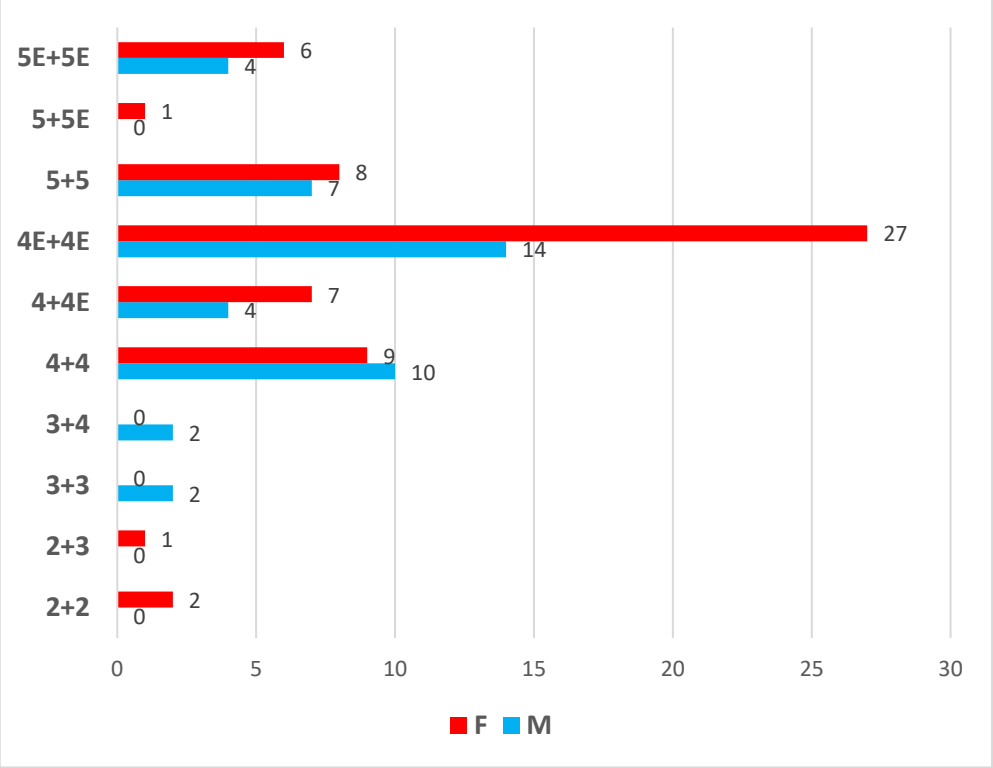

Graph 1- 1 - Comparative graph of the prevalence of the topographic types of the large palatal foramen in the male (n1=43) and female (n2=61) sublots. In both sublots maxillary 3rd molar edentations prevail but they are more numerous in the female sublot.

In the overall group most cases had type 4E bilaterally, i.e. GPM located medial to the edentulous site of maxillary M3 (39.42%). Only one case (0.96%) had GPM located distal to M3 (dentate but contralaterally edentulous) and associated types 2 and 3, i.e. GPM located medial to M2 associated contralaterally with the location at the interproximal septum between maxillary M2 and M3.

In the subgroup of males (n1=43) most cases presented, as in the general group, type 4E bilaterally, i.e. GPM located medial to the edentulous site of maxillary M3 (32.56%). There were no "2+2", "2+3" and "5+5E" combinations.

In the female subgroup (n2=61) the majority of cases had type 4E bilaterally, so GPM located medial to the edentulous site of maxillary M3 (44%). In only one case (2%) were GPM located distal to M3 (dentate but contralaterally edentulous) and associated types 2 and 3, so GPM located medial to M2 associated contralaterally with location at the interproximal septum between maxillary M2 and M3. There were no combinations of "3+3" and "3+4" types.

1.3.2 Results in the dentate sublot

In the overall group (N=104) there were 41 bilaterally dentate cases in 21 males (n3) and 20 females (n4). The dental topography of GPM in the dentate sublot is shown in the following table.

	2+2	2+3	3+3	3+4	4+4	5+5
M	0	0	2	2	10	7
F	2	1	0	0	9	8
TOTAL	2	1	2	2	19	15

Tab. 1- 2 - Bilateral distribution of topographic types of the large palatal hole, referred to upper molars, in the sublot of dentate cases. Bilateral asymmetry was recorded in 3/41 cases (7.31%), one case (2.43%) with GPM at M2 and M2/M3 septal level respectively and two other cases (4.87%) with M3-M2/M3 topographic combination. M: male; F: female.

1.3.3 Results in the edentulous sublot

In 63 cases we showed distal maxillary edentulousness, in which the position of the GPM could not be topographically referred to maxillary molars. There were 22 such male cases and 41 female cases. There were 51 bilateral edentations, 3 distal edentations on the right side and 9 such edentations on the left side.

1.4 Results - Topography of the large palatine hole in the hard palate

We have documented the values for the distances between the GPM and the incisive fossa of the hard palate (**tab.1-3**) and between the GPM and the posterior nasal spine (**tab.1-4**), respectively. Regarding the first of these two variables, I note that the range of morphometric variation was wider in female cases. The values obtained for the GPM-posterior nasal spine distance had lower averages in females.

	R-min	R-max	R-mean	L-min	L-max	L-mean
M	36,62	45,89	40,58	36,55	47,82	40,86
F	32,54	46,38	38,63	31,78	49,03	38,3
TOTAL	32,54	46,38	39,25	31,78	49,03	39,12

Tab. 1- 3 - Reference values in the investigated group (N=72) regarding the distance (mm) between the large palatal hole and the incisive fossa of the bony palate. "min" - minimum distance; "max" - maximum distance; "mean" - average value; M - male cases; F: female cases; R - right side; L - left side.

	R-min	R-max	R-mean	L-min	L-max	L-mean
M	14,77	20,19	17,27	14,76	20,64	17,44
F	13,53	19,42	16,21	12,97	19,65	16,38
TOTAL	13,53	20,19	16,56	12,97	20,64	16,72

Tab. 1- 4 - Reference values in the investigated group (N=72) regarding the distance (mm) between the large palatal hole and the posterior nasal spine. "min" - minimum distance; "max" - maximum distance; "mean" - average value; M - male cases; F: female cases; R - right side; L - left side.

The values of the distances determined between the GPM and the incisal fossa were grouped into types A-D. In the overall group (N=72), on the right side, the resulting prevalences were: type A - 3.47%, type B - 28.47%, type C - 15.97% and type D - 2.08%. On the left side, type A was identified in 6.94%, type B in 26.39%, type C in 13.89% and type D in 2.78%.

In men (N_B =23) we did not identify type A (distance < 35 mm), type B (35-40 mm) was present on the right in 12 cases and on the left in 13 cases, type C (40-45 mm) was present on the right in 10 cases and on the left in 7 cases, and type D (>45 mm) was identified on the right in one case and on the left in 3 cases. In women (N_F =49) type A (distance < 35 mm) was present on the right in 5 cases and on the left in 10 cases, type B (35-40 mm) was present on the right in 29 cases and on the left in 25 cases, type C (40-45 mm) was present on the right in 13 cases and on the left in 13 cases, and type D (>45 mm) was identified on the right in 2 cases and on the left in one case.

Bilateral asymmetry of value group types for GPM - incisor fossa distance in males (N_M =23) was identified in 13.04%; bilateral symmetric type A was not detected, bilateral symmetric type B was present in 52.17%, bilateral symmetric type C occurred in 30.43% and type D in 4.35% . In females (N_F =49) bilateral asymmetry was identified in 26.53%; bilateral symmetric type A was detected in 10.2%, bilateral symmetric type B was present in 44.9%, bilateral symmetric type C occurred in 18.37% and type D did not show bilateral symmetry.

In the overall group (N=72) there were 144 bilateral determinations of distances between the GPM and the posterior nasal spine. The values obtained were grouped into 8

types with the following prevalences: type 1 - 3.47%, type 2 - 6.94%, type 3 - 25%, type 4 - 25.69%, type 5 - 21.53%, type 6 - 10.42%, type 7 - 5.56% and type 8 - 1.39%.On the right side, in the overall group (N=72) the types for the distance GPM - posterior nasal spine, had the prevalences: type 1 - 1.39%, type 2 - 9.72%, type 3 - 22.22%, type 4 - 30.56%, type 5 - 23.61%, type 6 - 8.33%, type 7 - 2.78% and type 8 - 1.39%.

1.5 Discussions

The hard palate is made by the palatine processes of the maxillary bones and the horizontal laminae of the palatine bones. The palatal vault is completed on the sides by the alveolar processes of the two palatine bones. An important anatomical landmark of the posterior palate in dentistry is the GPM which lies between the horizontal blade of the palatine bone and the maxillary bone.

Changes in the alveolar ridge, and subsequently the palatal arch, may be due to physiological resorption with age, total or partial dentures, traumatic extractions or changes in bone metabolism. These factors predispose to morphological variations of the alveolar ridge and limit the usefulness of distances between the GPM and the buccal alveolar wall in the live localization of the GPM.

2 Anatomo-imaging investigations of the nasopalatine duct

2.1 Introduction

The anterior maxilla is a region of interest for clinicians performing various oral and maxillofacial surgery procedures, such as insertion of endosseous implants, enucleation of wisdom teeth, orthognathic surgery, and extraction of impacted and supernumerary teeth. A good knowledge of the morphological details of the anterior maxilla is important for successful surgical protocols, including the avoidance of neurovascular complications. Morphological estimation of the NPC is useful to clinicians for implant insertion.

Although the NPC is one of the most important anatomical structures in the premaxilla, there is little documentation available on the anatomical variations, dimensions and morphology of the NPC. Oral implant surgery at the edentulous premaxilla is often challenging due to the aesthetic, phonetic and biomechanical implications.

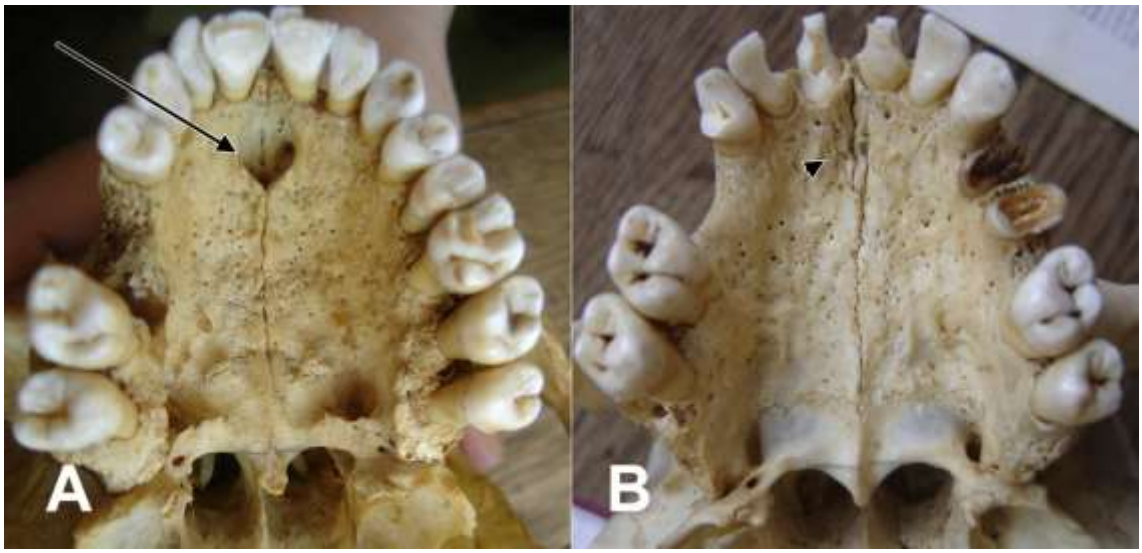

Fig. 2- 1 - Dried skulls, lower view of hard palate. (A) Anatomically defined incisive fossa (arrowhead), proper nasopalatine canals discernible. (B) Incisive fossa morphologically absent (arrowhead), numerous fine canaliculi open at this level.

I noticed the hard palate on the dry skulls. We identified a specimen that did not show the usual anatomical morphology (**Fig. 2-1**): the incisive fossa was absent and numerous canaliculi, and not a morphologically configured NPC, opened through foramina in the respective anatomical site. We thus hypothesized that the CNP may also be absent. Thus, we designed an anatomical-imaging study to identify anatomical variables of the CNP, including its presence or absence. I consider that there is no universally accepted terminology for CNP/CI.

The nasopalatine canal (incisive canal of the premaxilla) has been assigned different morphologies in the frontal plane, one being the "Y" shape with two upper arms (own CNP). The nasopalatine canal with a "Y" morphology has the two upper arms separated by a bony wall that is different from the nasal septum.

2.2 Material and method

2.2.1 Study lots

2.2.1.1 Batch used in the nasopalatine duct study

To assess CNP/CI variability we used a retrospective batch of archived Cone Beam CT (CBCT) records from 89 patients, 38 male (42.69%) and 51 female (57.3%).

2.2.1.2 *Batch used in the nasomaxillary ridge study*

To assess the variability of nasomaxillary ridge we used a retrospective batch of archived CBCT records from 41 patients, 11 male (26.82%) and 30 female (73.18%).

2.2.2 Research method

We performed a retrospective CBCT study of archived patient files from the two groups. Cases were scanned with an iCat (Imaging Sciences International [Hatfield, PA, USA]) with settings: resolution 0.250, FOV 130, image matrix size 640 x 640. Patients were positioned according to the manufacturer's recommendations. Scanned data were exported as *.dcm files and evaluated with Planmeca Romexis Viewer 3.5.0.R software, as in previous studies [[20] and with Blu Sky Plan software (BlueSkyBio.com). We evaluated both two-dimensional planar sections and three-dimensional renderings. Patients gave informed consent for the use of their data in the research, provided they were anonymized.

2.2.3 Documented anatomical variables

2.2.3.1 *Morphological variables of the nasopalatine duct*

In the NPC study we looked at the following anatomical variables:

- presence or absence of this channel;
- the number of superior orifices (nasopalatine holes);
- the number of lower openings (incisor hole);
- Nasopalatine canals proper (superior): position in frontal plane (parallel, Y-shaped), number, intracanal septa leading to secondary canaliculi.

2.2.3.2 *Anatomical variables of the nasomaxillary or septo-premaxillary ridge*

In the batch of 41 anatomically documented cases for nasomaxillary or septopremaxillary ridge (NMC/SPMC) we followed the following anatomical variables:

- median or sloping placement of the CNM/CSPM;
- the length of this ridge: either short ridge not descending into the CNP or long ridge descending into the CNP;
- the presence or absence of the CNP.

2.3 Results

2.3.1 Anatomo-imaging study of the nasopalatine duct

We detected a number of individual variations in CNP/CI in the investigated group (N=89). These corresponded to the following types and subtypes that we have defined below.

CNP types:

- type I - CNP/CI present, with 2 nasopalatine holes and 1 GI;
- type II - CNP/CI absent, 2 nasopalatine holes, 1 GI;
- type III - CNP/CI present, unique, with 1 nasopalatine hole and 1 GI;
- type IV - CNP/CI present, 3 nasopalatine holes, two lateral and one medial, 1 GI;
- type V - CNP/CI absent, nasopalatine holes absent, 1 incisive hole, blind.

Type I showed the following subtypes in the investigated batch:

- subtype Ia - CNP in "Y", without secondary canaliculi;
- subtype Ib - "Y" NPC with secondary canaliculi (sagittal intracanal septum);
- subtype Ic - "Y" NPC with secondary canaliculi (coronal septum) in a single NPC of its own;
- Id subtype - "Y" NPC with secondary canaliculi (coronal septum) in both proper NPCs;
- subtype Ie - NPC in "Y", with blind median channel between own NPC;
- subtype If - NPC with parallel upper arms separated by septa;
- Ig- CNP subtype present, 2 nasopalatine holes, 1 GI, no septum.

Type III had two subtypes:

- subtype IIIa - median nasopalatine hole, inferior to CNM/CSPM;
- subtype IIIb - medial nasopalatine hole, lateral to deviated CNM/CSPM.

The distribution of cases by type of NPC showed the prevalence of type I (66.29%) in the investigated group (N=89) (**Figure 2-1**). Only 2 cases in the overall group (2.25%) showed type II - absent NPC with two nasopalatine holes at the nasal tip and one GI. In 17.87% we identified type III NPC - single, tubular canal with one hole at the extremities. Type IV NPC was identified in 3 cases (3.37%), Type V NPC was present in 9 cases (10.11%). Type I NPC was also prevalent in the male subtype (N1=35) and female subtype (N2=54).

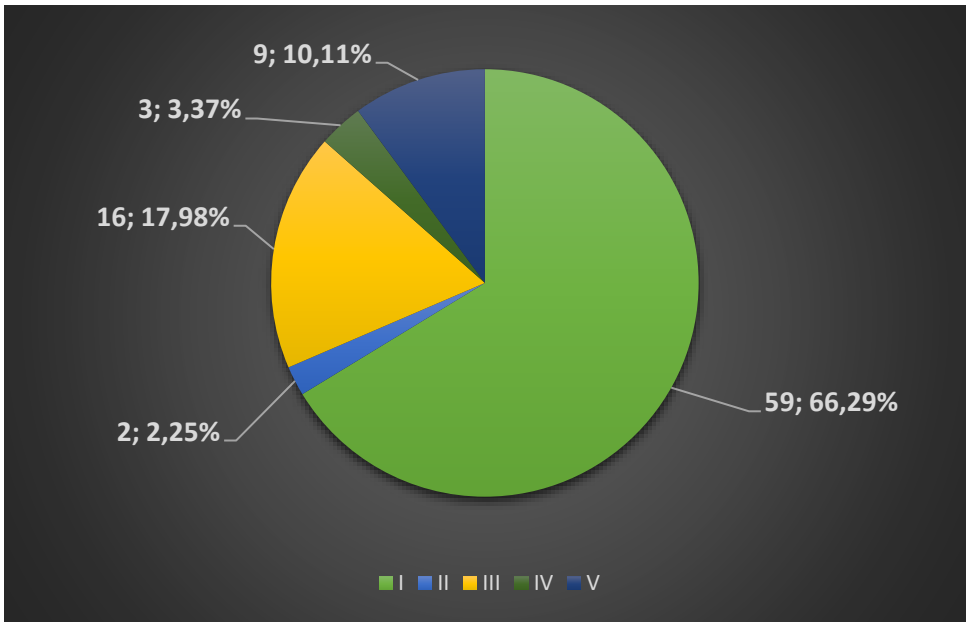

Graph 2- 1 - Prevalence of cases by type of nasopalatine duct in the studied group (N=89).

2.3.2 Other anatomical variations associated with the nasopalatine duct

2.3.2.1 Incisor accessory foramina

Fig. 2- 4 - Three-dimensional rendering. Lower view of the incisal hole. Two openings located immediately to the right of the incisal foramen (arrows) communicate with another opening (arrowhead) on the right side of the incisal fossa.

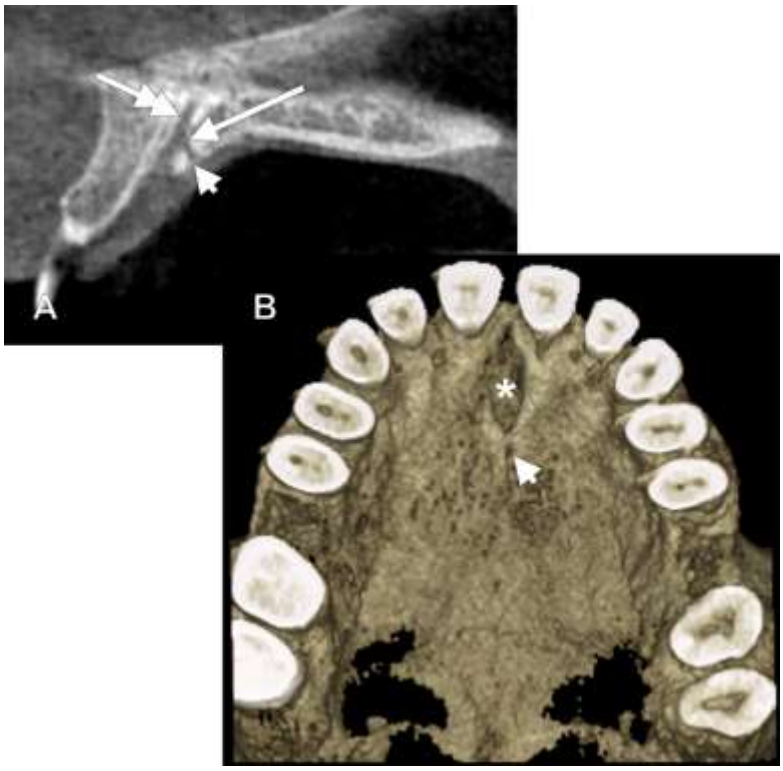

Fig. 2- 5 - Posterior median incisor foramen. A: Sagittal CBCT section. B: three-dimensional rendering. From the right proper incisive canal (double-tip arrow) starts a posteroinferior canaliculus (arrow) that opens to a median foramina (arrowhead) located immediately posterior to the incisive foramen (*).

2.3.2.2 Nasomaxillary or septo-premaxillary ridge

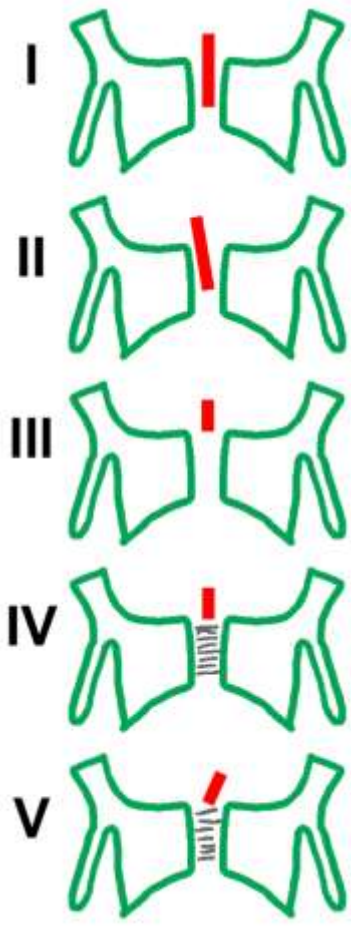

Fig. 2- 6 - Anatomical diagrams of types I-V of nasomaxillary (septopremaxillary) ridge. See description in text.

On a batch of 41 CBCT records we identified 5 main types of nasomaxillary crest (NMC) or septo-premaxillary crest (SPMC):

- type I - CNM/CSPM long median, descends into CNP;
- type II - long sloping CNM/CSPM, descending into CNP;
- type III - CNM/CSPM short median, does not descend into CNP;
- type IV - CNM/CSPM short median, CNP absent;
- type V - CNM/CSPM short inclined, CNP absent.

The distribution of morphological patterns in the overall batch is shown in the following graph. In 51.22% of cases we identified type I (long median CNM/CSPM separating proper NPC/CI). In 21.95% we identified type III (short median CNM/CSPM not separating proper NPC/CI - single NPC). In 19.51% we obtained evidence for type V, with deviated short CNM/CSPM and absent NPC/CI.

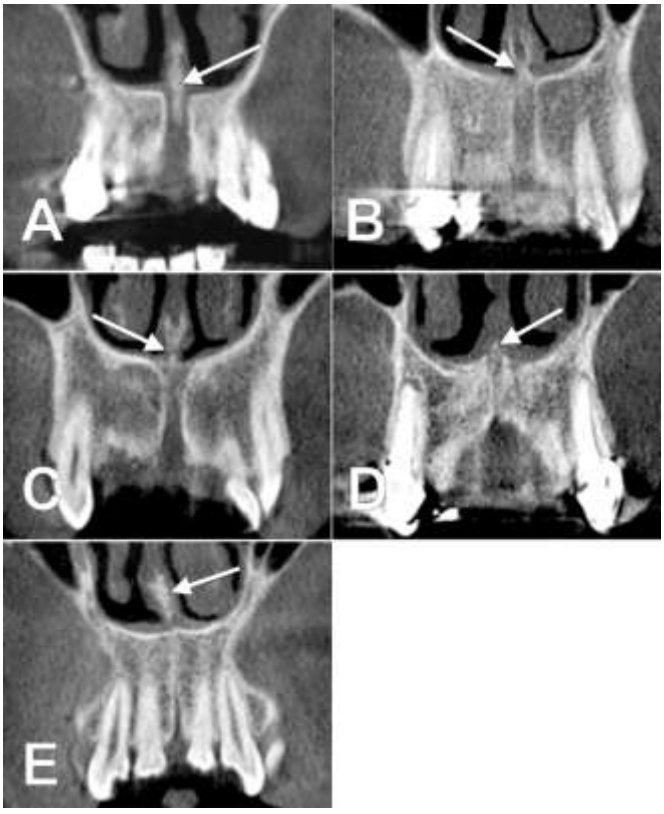

Fig. 2- 7 - Coronal CBCT sections. Morphological possibilities of the nasomaxillary/septopremaxillary ridge. A. type I. B. type II. C: type III. D. type IV. E. type V.

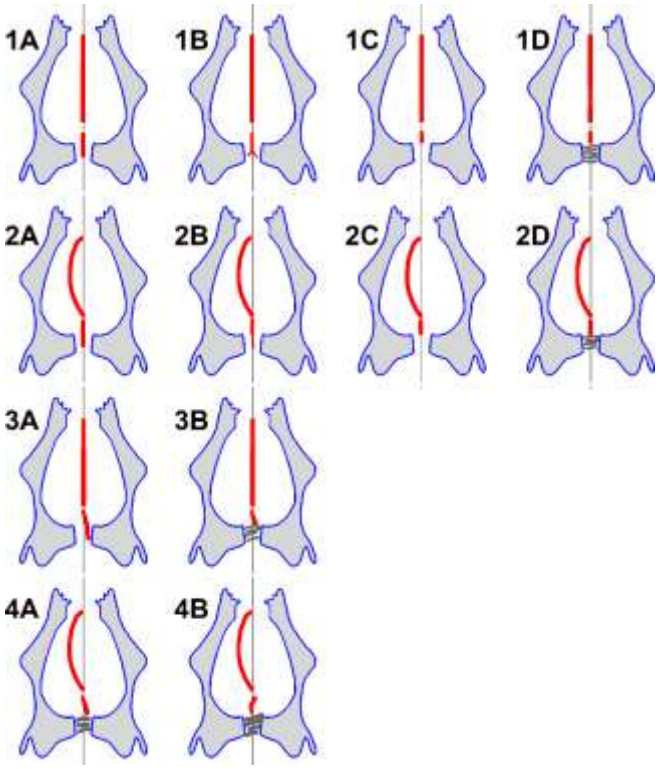

Fig. 2- 8 - Diagrams of the variational possibilities of the nasomaxillary ridge (septo-premaxillary crest) identified by personal study. Types of morphological association: "1A" vertical nasal septum, vertical nasomaxillary ridge, descended between proper nasopalatine canals; "1B" vertical nasal septum, vertical nasomaxillary ridge, descended between proper nasopalatine canals, inferior bifid; "1C" vertical nasal septum, short vertical nasomaxillary ridge, above nasopalatine canal; '1D' vertical nasal septum, short vertical nasomaxillary ridge, nasopalatine duct absent; '2A' deviated nasal septum, vertical nasomaxillary ridge, descended between the proper nasopalatine canals; '2B' deviated nasal septum, vertical nasomaxillary ridge, extended with a thin septum between the proper nasopalatine canals; '2C' deviated nasal septum, short vertical nasomaxillary ridge, superior to nasopalatine duct; '2D' deviated nasal septum, short vertical nasomaxillary ridge, nasopalatine duct absent; '3A' vertical nasal septum, deviated nasomaxillary ridge, descended between proper nasopalatine ducts; '3B' vertical nasal septum, deviated nasomaxillary ridge, short, nasolabial canal absent; '4A' deviated nasal septum with ipsilateral sloping nasomaxillary ridge; '4B' deviated nasal septum with contralateral sloping nasomaxillary ridge.

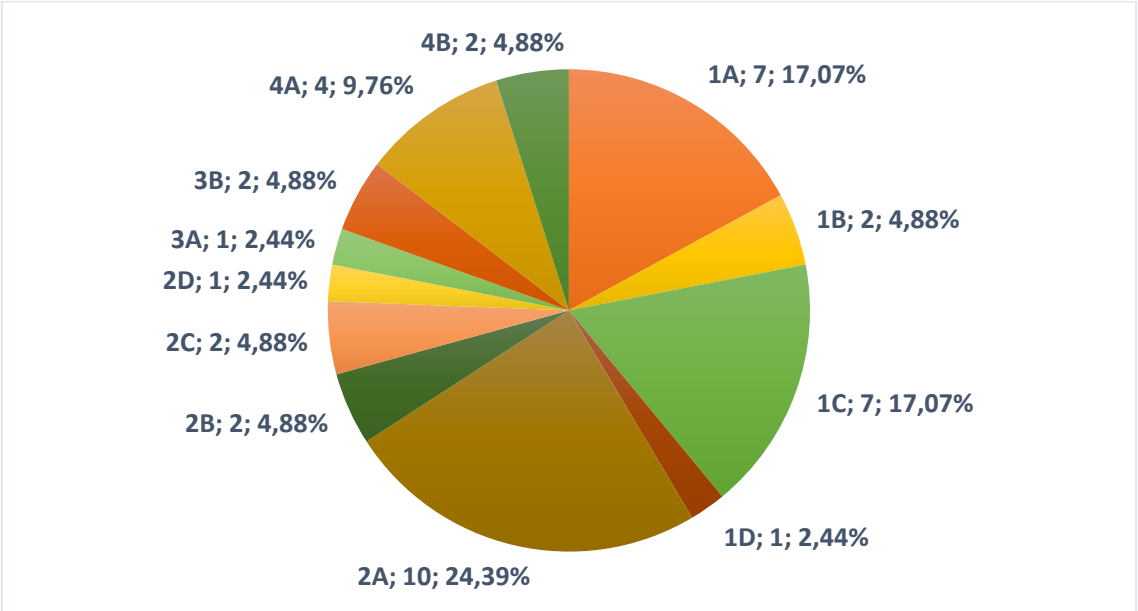

Graph 2- 2 - Distribution of anatomical variants (type;number;%) of nasomaxillary (septo-premaxillary) ridge in the investigated group (N=41).

2.4 Discussions

2.4.1 Anatomical variability of the nasopalatine duct

Due to the close anatomical relationship between the NPC and the roots of the maxillary central incisors, careful radiological analysis of the bone substrate is required when considering the insertion of implants in the premaxilla. Dental rehabilitation with osseointegrated dental implants in the anterior maxilla has become a common treatment in dental practice..

The nasopalatine canal (NPC), or incisive canal (IC) of the maxilla, is a bony canal connecting the nasal fossae with the palate, hence its name. Being located palatally of the maxillary central incisors it is also called the incisive canal. A distinction must be made between the NPC and the nasopalatine duct, the latter being an epithelial structure within the NPC..

As a rule, NPC originates bilaterally from the nasal infundibulum, which are the upper funnel-shaped openings placed on the sides of the nasal septum in the anterior part of the nasal floor. The superior openings of the NPC are separated by the nasomaxillary ridge. Sagittally, the CNP descends slightly obliquely; coronally, the two upper arms of the CNP join approximately midway along the total length of the CNP and continue inferiorly as a single canal. The nasopalatine canal terminates at the inferior orifice, this palatal opening is called the incisive foramen (GI), double in 2% of cases, and located immediately deep to the incisive papilla of the anterior palatine mucosa Nasomaxillary ridge

The different anatomical possibilities of CNM/CSPM that we identified showed that CNP/CI also has different possible morphologies in coronal sections, and not just the shape of the letter "Y". This is in agreement with various previously published studies but also points to an overlooked possibility, that of the absence of CNP/CI. This latter aspect I have documented through another research in my PhD thesis.

3 Anatomo-imaging studies of the greater palatine canal

3.1 Introduction

CPM anatomy is of clinical interest in dentistry, oromaxillofacial surgery and otolaryngology... Local anaesthesia is administered at the CPM, endosseous implants can be inserted, and syngnathic surgical procedures as well as Le Fort I orthognathic

osteotomies are performed. Anesthesia of the maxillary nerve via the CPM is a very good method of achieving anaesthesia in the jaw.

3.2 Material and method

We conducted a retrospective CBCT study of archived files of 50 patients, 18 male and 32 female. Cases were scanned with an iCat (Imaging Sciences International [Hatfield, PA, USA]) with settings: resolution 0.250, FOV 130, image matrix size 640 x 640. Patients were positioned according to the manufacturer's recommendations. Scanned data were exported as *.dcm files and evaluated with Planmeca Romexis Viewer 3.5.0.R software, as in previous studies, and Blu Sky Plan software (BlueSkyBio.com). We evaluated both two-dimensional planar sections and three-dimensional renderings. Patients gave informed consent for the use of their data in the research, subject to anonymization.

3.2.1 Documented anatomical variables

In the CBCT anatomy study of CPM we documented the following anatomical variables: (1) vertical angulation of the CPM in the frontal plane (coronal plane), documented on coronal sections, at the exit of the canal (GPM); (2) vertical angulation of the CPM in the sagittal plane, documented on sagittal sections (we made the determination in the inferior, angulated portion of the CPM, inferior to the FPP); (3) luminal diameter of the CPM, measured antero-posteriorly, at mid-length of the CPM, at maximally spaced points, at the level of the posterior insertion of the CNI; (4) lateral ratio of the CPM to either maxillary M3 (or inclusion of M3 respectively), to SM, or edentulous alveolar bone; (5) changes in angulation of the CPM in the coronal plane; (6) changes in angulation of the CPM in the sagittal plane. For variables "5" and "6" we defined the following morphological types: type 0 - straight CPM; type 1 - CPM changes direction only once; type 2 - two direction changes; type 3 - three direction changes.

3.3 Results

3.3.1 Variable (1) - angulation of the large palatal canal in the coronal plane

CPM angle to vertical, coronal plane - right side

On the right side, the CPM angle with the vertical to its inferior orifice was open to the side in 8/50 cases (16%), 3 male and 5 female. The lateral angulation of the right CPM averaged 3.68^{o} (min.0.3^{o} - max.14.31^{o}). Medial angulation was identified in 42/50 cases

(84%), 27 male and 15 female. Medial angulation of the right CPM averaged 5.36º (min.0.64º - max.15.38º).

CPM angle to vertical, coronal plane - left side

On the left side, the CPM angle with the vertical, towards its inferior orifice, was open to the side in 13/50 cases (26%), 4 male and 9 female. The lateral angulation of the left CPM averaged 3.66º (min.0.64º - max.15.38º). Medial angulation was identified in 37/50 cases (74%), 14 male and 23 female (**graph 2**). Medial angulation of the left CPM averaged 5.83º (min.1.09º - max.15.25).º

Bilateral comparison of CPM angulation in the coronal plane

The right and left large palatal canals were considered coronally parallel if one had lateral angulation to the GPM and the contralateral one had medial angulation . We identified parallel MPCs in 17/50 cases (34%). The large palatal canals were considered convergent inferiorly, towards the GPM, when they showed bilateral medial angulation. We identified inferiorly convergent CPMs in 31/50 cases (62%), 11 male and 20 female. Large palatal canals were considered inferiorly divergent if they had bilateral lateral angulation. We identified inferiorly divergent CPMs in 2/50 cases (4%), both female.

3.3.2 Variable (2) - sagittal angulation of the large palatine canal

All documented CPMs had an anterior-inferior trajectory in the sagittal plane. In the overall group, the mean value of the antero-inferior angle of the CPM was on the right side 28.54º (min.11.81º - max.41.09º) and on the left side 27.13º (min.15.45º - max.38.55º). On the right side, the mean value of the sagittal angulation of the CPM in males was 25.51º (min.11.81-º max.37,22º) and in women 30,24º (min.20,97º - max.41,09º). On the left side, the mean value of the sagittal angulation of the MPC was 23,93º (min.15,45-º max.35,59º) and in women 28,93º (min.17,49º - max.38,55º).

3.3.3 Variable (3) - luminal diameter of the large palatine canal

The mean luminal diameter of the CPM on the right side was 2.98 mm. The mean luminal diameter of the left CPM was 3.05 mm. The minimum MPC diameter was 1.77 mm on the right side and 1.68 mm on the left side, these values were determined in the same female case. The maximum diameter of the MPC was 5.26 mm on the right side and 4.7 mm on the left side.

3.3.4 Variable (4) - lateral ratios of the large palatal hole

We defined the following types of GPM according to its immediate lateral relationship: (a) type 1, alveolar - relationship to alveolar bone (either dentate alveolar base, 1d, or edentulous bone, 1e); (b) type 2, sinus - relationship to alveolar recess of maxillary sinus; (c) type 3, dental - relationship to M3 included. These anatomical types showed in most cases (42/50 cases, 84%) bilateral symmetry. We identified type 1d bilaterally in 9/50 cases (18%). Type 1e was evident bilaterally in 19/50 cases (38%). Type 2, sinus, was evident in 5/50 cases (10%). Type 3 - immediate lateral GPM ratio with maxillary M3 included, was identified bilaterally in 9/50 cases (18%).

On the right side the immediate lateral GPM ratios were in 13/50 cases type 1d, in 22/50 cases type 1e, in 5/50 cases type 2, and in 10/50 cases type 3 .

On the left side the immediate lateral GPM ratios were in 10/50 cases type 1d, in 20/50 cases type 1e, in 8/50 cases type 2, and in 12/50 cases type 3.

We have highlighted the bilateral asymmetry for the combinations of types 1d/1e, 1d/2, 1e/2, 1d/3 and 1e/3. We found bilateral asymmetry of anatomical types determined in one case (2%) for the type combinations 1e/1d, 1d/2, 1e/3 respectively. In 2/50 cases we found bilateral combination of 1e/2 types (4%). In 3/50 cases we found bilateral combination of 1d/3 types (6%).

types	*1e/1e*	*1d/1d*	*2/2*	*3/3*	*1e/1d*	*1d/2*	*1e/2*	*1d/3*	*1e/3*
M	8	3	2	3	1	0	0	1	0
F	11	6	3	6	0	1	2	2	1
Total	**19**	**9**	**5**	**9**	**1**	**1**	**2**	**3**	**1**

Tab. 3- 1 - Bilateral combinations of types of immediate lateral ratio of the large palatal foramen. Distribution by genus and in the general batch.

3.3.5 Variables (5) and (6) - changes in angulation/direction of the large palatal canal

We anatomically assessed 100 CPM, 50 on the right side and 50 on the left side, for coronal plane direction/angulation changes (variable 5). Of these on the right, 34

CPM type 0 (rectilinear canal) were identified, and on the left - 33 CPM type 0. Type 1 V5 CPM, with a change in direction, was present at 10 CPM on the right side and 11 CPM on the left side. Type 2 V5 CPM, with two steering changes, was present at 6 CPM from the right side and 5 CPM from the left side. Type 3 V5 CPM, with three steering changes, was present at 1 CPM from the left side.

Of the 100 CPMs analysed bilaterally for angulation in the sagittal plane (change of direction in the sagittal plane, variable V6), we did not record type 3 - three changes of direction. On the right side we identified 36 type 0 CPMs (rectilinear channel), and on the left - 39 type 0 CPMs. Type 1 V6 CPM, with one direction change, was present at 7 CPM on the right side and 5 CPM on the left side. Type 2 V6 CPM, with two steering modifications, was present at 7 CPM from the right side and 6 CPM from the left side.

3.4 Discussions

The pterygopalatine fossa (PPF) is an inverted pyramid-shaped fossa located in the lateral norm of the skull, medial to the infratemporal fossa. The pterygopalatine fossa communicates with the middle cranial fossa through the round hole and inferiorly with the posterior palatine region through the CPM. In the literature there are differences in the determination of variables such as the length of the CPM: some authors have determined this parameter from the GPM to the pterygoid (vidian) canal open in the PPF, while others have considered the upper end of the CPM at the level of the "lower portion of the PPF". the latter parameter being subjective.

In addition, caution should be exercised to avoid possible damage to the medial wall of the maxillary sinus if the inclination of the inserted dental implant body is almost perpendicular to the plane through the hamolar incision and the incisal papilla.

3.4.1 Lateral structural relationships of the large palatine foramen

The posterior maxilla is a particularly difficult area to place an endodontic implant due to several factors. Some of the factors on which the insertion of an endosseous implant in the posterior maxillary region depends are: (a) difficult access; (b) limited visibility; (c) reduced space between the alveolar-dental arches; (d) bone resorption combined with antral hyperpneumatization; poor bone quality (thin layer of compact

bone). To these factors of difficulty in the insertion of a posterior maxillary implant are added, as my study demonstrates, the vicinity with GPM.

Conclusions the Doctoral Thesis

1. If on one side of the median plane the large palatine hole has a certain topographic pattern, it is not necessarily repeated on the opposite side of the median plane.
2. There are various anatomical possibilities of the nasomaxillary/septopremaxillary ridge that can be identified primarily in coronal sections.
3. The anatomical possibilities of the nasopalatine duct are diverse. Therefore, a typical description of this canal cannot be assumed, especially during the anatomical education of dental students. The absence of the nasopalatine canal has not been identified in previous studies.
4. The morphology and geometry of the large palatine canal are individually variable and do not consistently follow bilateral symmetry.
5. Anatomical investigations of the large palatine foramen can be carried out by different methodologies on different sized batches. Therefore, results are difficult to standardise.
6. Identification of anatomical features on imaging sections must be done carefully to avoid misinterpretation.
7. It would be useful to include in the anatomical education of dental school students the use of CBCT analysis software useful after graduation in the dental office.
8. Interpretation of ductal and foraminal anatomy must be done on a case-by-case basis and not considered within the framework of usual templates.

Bibliography of the Doctoral Thesis

1. Abrams AM, Howell FV, Bullock WK (1963) Nasopalatine cysts. Oral Surg Oral Med Oral Pathol, 16:306-332. doi:10.1016/0030-4220(63)90295-0
2. Acar B, Kamburoglu K (2015) Morphological and volumetric evaluation of the nasopalatine canal in a Turkish population using cone-beam computed tomography. Surg Radiol Anat, 37:259-265. doi:10.1007/s00276-014-1348-9

3. Ajmani ML (1994) Anatomical variation in position of the greater palatine foramen in the adult human skull. J Anat, 184 (Pt 3):635-637.
4. Al-Amery SM, Nambiar P, Jamaludin M, et al. (2015) Cone beam computed tomography assessment of the maxillary incisive canal and foramen: Considerations of anatomical variations when placing immediate implants. PLoS One, 10:e0117251. doi:10.1371/journal.pone.0117251
5. Al Dayeh AA, Herring SW (2014) Cellular proliferation in the nasal septal cartilage of juvenile minipigs. J Anat, 225:604-613. doi:10.1111/joa.12237
6. Aoun G, Nasseh I, Sokhn S, et al. (2015) Analysis of the greater palatine foramen in a Lebanese population using cone-beam computed tomography technology. J Int Soc Prev Community Dent, 5:S82-88. doi:10.4103/2231-0762.171594
7. Aoun G, Zaarour I, Sokhn S, et al. (2015) Maxillary nerve block via the greater palatine canal: An old technique revisited. J Int Soc Prev Community Dent, 5:359-364. doi:10.4103/2231-0762.165930
8. Awad AS, Tohamy HMA, Gadallah HN, et al. (2020) Role of multi-detector ct in analysis of the greater and lesser palatine foramina. 51:1-14.
9. Ayoub N, Thamboo A, Hwang PH, et al. (2017) Radioanatomic study of the greater palatine canal relevant to endoscopic endonasal surgical landmarks. Otolaryngol Head Neck Surg, 157:731-736. doi:10.1177/0194599817711883
10. Ayyildiz VA, Dursun A (2021) Evaluation of hard palate asymmetry in Turkish population.
11. Bahsi I, Orhan M, Kervancioglu P (2017) A sample of morphological eponym confusion: foramina of stenson/stensen. Surg Radiol Anat, 39:935-936. doi:10.1007/s00276-017-1835-x
12. Bahsi I, Orhan M, Kervancioglu P, et al. (2019) Morphometric evaluation and clinical implications of the greater palatine foramen, greater palatine canal and pterygopalatine fossa on cbct images and review of literature. Surg Radiol Anat, 41:551-567. doi:10.1007/s00276-019-02179-x
13. Bahşi İ, Orhan M, Kervancıoğlu P, et al. (2019) Morphometric evaluation and clinical implications of the greater palatine foramen, greater palatine canal and pterygopalatine fossa on cbct images and review of literature. 41:551-567.
14. Barteczko K, Jacob M (2004) A re-evaluation of the premaxillary bone in humans. Anat Embryol (Berl), 207:417-437. doi:10.1007/s00429-003-0366-x
15. Benninger B, Andrews K, Carter W (2012) Clinical measurements of hard palate and implications for subepithelial connective tissue grafts with suggestions for palatal nomenclature. J Oral Maxillofac Surg, 70:149-153. doi:10.1016/j.joms.2011.03.066
16. Bodereau EF, Flores VY, Naldini P, et al. (2020) Clinical evaluation of the nasopalatine canal in implant-prosthetic treatment: A pilot study. Dent J (Basel), 8doi:10.3390/dj8020030
17. Bornstein MM, Balsiger R, Sendi P, et al. (2011) Morphology of the nasopalatine canal and dental implant surgery: A radiographic analysis of 100 consecutive patients using limited cone-beam computed tomography. Clin Oral Implants Res, 22:295-301. doi:10.1111/j.1600-0501.2010.02010.x
18. Bush JO, Jiang R (2012) Palatogenesis: Morphogenetic and molecular mechanisms of secondary palate development. Development, 139:231-243. doi:10.1242/dev.067082
19. Cagimni P, Govsa F, Ozer MA, et al. (2017) Computerized analysis of the greater palatine foramen to gain the palatine neurovascular bundle during palatal surgery. Surg Radiol Anat, 39:177-184. doi:10.1007/s00276-016-1691-0
20. Carstocea L, Rusu MC, Matesica DS, et al. (2019) Air spaces neighbouring the infraorbital canal. Morphologie, doi:10.1016/j.morpho.2019.07.002
21. Cavallaro J, Tsuji S, Chiu TS, et al. (2016) Management of the nasopalatine canal and foramen associated with dental implant therapy. Compend Contin Educ Dent, 38:367-372; quiz 374.

22. Chauhan JS, Sharma S (2019) Lag screw fixation of the premaxilla during bilateral cleft lip repair. J Craniomaxillofac Surg, 47:1881-1886. doi:10.1016/j.jcms.2019.11.015
23. Chrcanovic BR, Custodio AL (2010) Anatomical variation in the position of the greater palatine foramen. J Oral Sci, 52:109-113.
24. Dadgarnia MH, Shahbazian H, Behniafard N, et al. (2016) Epinephrine injection in greater palatine canal: An alternative technique for reducing hemorrhage during septoplasty. J Craniofac Surg, 27:548-551. doi:10.1097/SCS.0000000000002413
25. Das S, Kim D, Cannon TY, et al. (2006) High-resolution computed tomography analysis of the greater palatine canal. Am J Rhinol, 20:603-608. doi:10.2500/ajr.2006.20.2949
26. Dave MR, Yagain VK, Anadkat S (2013) A study of the anatomical variations in the position of the greater palatine foramen in adult human skulls and its clinical significance. Int J Morphol, 31:578.
27. Diewert VM, Wang KY (1992) Recent advances in primary palate and midface morphogenesis research. Crit Rev Oral Biol Med, 4:111-130. doi:10.1177/10454411920040010201
28. Douglas R, Wormald PJ (2006) Pterygopalatine fossa infiltration through the greater palatine foramen: Where to bend the needle. Laryngoscope, 116:1255-1257. doi:10.1097/01.mlg.0000226005.43817.a2
29. Dursun A, Ozturk K, Albay S (2018) Development of hard and soft palate during the fetal period and hard palate asymmetry. J Craniofac Surg, 29:2358-2362. doi:10.1097/SCS.0000000000005016
30. Duruel O, Kulkarni V, Ataman-Duruel ET, et al. (2019) Radio-morphometric evaluation of greater palatine canal and pterygopalatine fossa component: Maxillary anesthetic implications. J Craniofac Surg, 30:863-867. doi:10.1097/SCS.0000000000005260
31. Etoz M, Sisman Y (2014) Evaluation of the nasopalatine canal and variations with cone-beam computed tomography. Surg Radiol Anat, 36:805-812. doi:10.1007/s00276-014-1259-9
32. Fawcett E (1911) The development of the human maxilla, vomer, and paraseptal cartilages J Anat Physiol, 45:378-405.
33. Feneis H, Dauber W. Pocket atlas of human anatomy: Based on the international nomenclature. 4th ed. Stuttgart; New York: Thieme; 2000.
34. Fernandez-Alonso A, Suarez-Quintanilla JA, Muinelo-Lorenzo J, et al. (2014) Three-dimensional study of nasopalatine canal morphology: A descriptive retrospective analysis using cone-beam computed tomography. Surg Radiol Anat, 36:895-905. doi:10.1007/s00276-014-1297-3
35. Fonseka MCN, Hettiarachchi P, Jayasinghe RM, et al. (2019) A cone beam computed tomographic analysis of the greater palatine foramen in a cohort of sri lankans. J Oral Biol Craniofac Res, 9:306-310. doi:10.1016/j.jobcr.2019.06.012
36. Friede H (1975) A histological and enzyme-histochemical study of growth sites of the premaxilla in human foetuses and neonates. Arch Oral Biol, 20:809-814. doi:10.1016/0003-9969(75)90058-8
37. Friede H, Morgan P (1976) Growth of the vomero-premaxillary suture in children with bilateral cleft lip and palate. A histological and roentgencephalometric study. Scand J Plast Reconstr Surg, 10:45-55. doi:10.1080/02844317609169745
38. Fukuda M, Matsunaga S, Odaka K, et al. (2015) Three-dimensional analysis of incisive canals in human dentulous and edentulous maxillary bones. Int J Implant Dent, 1:12. doi:10.1186/s40729-015-0012-4
39. Gibelli D, Borlando A, Dolci C, et al. (2017) Anatomical characteristics of greater palatine foramen: A novel point of view. Surg Radiol Anat, 39:1359-1368. doi:10.1007/s00276-017-1899-7
40. Gorurgoz C, Oztas B (2020) Anatomic characteristics and dimensions of the nasopalatine canal: A radiographic study using cone-beam computed tomography. Folia Morphol (Warsz), doi:10.5603/FM.a2020.0118

41. Gray H, Standring S, Anand N, et al. Gray's anatomy: The anatomical basis of clinical practice. 41 ed. London, UK: Elsevier; 2016.
42. Gray H, Williams PL, Gray H. Gray's anatomy. 37th ed. Edinburgh; New York: C. Livingstone; 1989.
43. Grymer LF, Pallisgaard C, Melsen B (1991) The nasal septum in relation to the development of the nasomaxillary complex: A study in identical twins. Laryngoscope, 101:863-868. doi:10.1288/00005537-199108000-00010
44. Hafeez NS, Ganapathy S, Sondekoppam R, et al. (2015) Anatomical variations of the greater palatine nerve in the greater palatine canal. 81:f14.
45. Hafkamp HC, Bruintjes TD, Huizing EH (1999) Functional anatomy of the premaxillary area. Rhinology, 37:21-24.
46. Hakbilen S, Magat G (2018) Evaluation of anatomical and morphological characteristics of the nasopalatine canal in a Turkish population by cone beam computed tomography. Folia Morphol (Warsz), 77:527-535. doi:10.5603/FM.a2018.0013
47. Hall BK, Precious DS (2013) Cleft lip, nose, and palate: The nasal septum as the pacemaker for midfacial growth Oral Surg Oral Med Oral Pathol Oral Radiol, 115:442-447. doi:10.1016/j.oooo.2012.05.005
48. Howard-Swirzinski K, Edwards PC, Saini TS, et al. (2010) Length and geometric patterns of the greater palatine canal observed in cone beam computed tomography. Int J Dent, 2010doi:10.1155/2010/292753
49. Huang H, Richards M, Bedair T, et al. (2013) Effects of orthodontic treatment on human alveolar bone density distribution Clin Oral Investig, 17:2033-2040. doi:10.1007/s00784-012-0906-y
50. Hwang SH, Seo JH, Joo YH, et al. (2011) An anatomic study using three-dimensional reconstruction for pterygopalatine fossa infiltration via the greater palatine canal. Clin Anat, 24:576-582. doi:10.1002/ca.21134
51. Iamandoiu AV, Ilie OC, Jianu AM, et al. (2021) The nasomaxillary or septo-premaxillary crest Med Evol, XXVII:386-391.
52. Iamandoiu AV, Mănoiu VS, Butucescu M, et al. (2021) A cone-beam computed tomography study of the greater palatine foramen. Med Evol, XXVII:266-273.
53. Iamandoiu AV, Mureșan AN, Rusu MCJA (2022) Detailed morphology of the incisive or nasopalatine canal. 1:75-85.
54. Ikuta CR, Cardoso CL, Ferreira-Junior O, et al. (2013) Position of the greater palatine foramen: An anatomical study through cone beam computed tomography images. Surg Radiol Anat, 35:837-842. doi:10.1007/s00276-013-1151-z
55. Iwanaga J, Voin V, Nasseh AA, et al. (2017) New supplementary landmark for the greater palatine foramen as found deep to soft tissue: Application for the greater palatine nerve block. Surg Radiol Anat, 39:981-984. doi:10.1007/s00276-017-1829-8
56. Jain NV, Gharatkar AA, Parekh BA, et al. (2017) Three-dimensional analysis of the anatomical characteristics and dimensions of the nasopalatine canal using cone beam computed tomography. J Maxillofac Oral Surg, 16:197-204. doi:10.1007/s12663-016-0879-5
57. Jensen OT (2014) Complete arch site classification for all-on-4 immediate function J Prosthet Dent, 112:741-751 e742. doi:10.1016/j.prosdent.2013.12.023
58. Jensen OT, Adams MW, Butura C, et al. (2015) Maxillary v-4: Four implant treatment for maxillary atrophy with dental implants fixed apically at the vomer-nasal crest, lateral pyriform rim, and zygoma for immediate function. report on 44 patients followed from 1 to 3 years.J Prosthet Dent, 114:810-817. doi:10.1016/j.prosdent.2014.11.018
59. Jensen OT, Cottam JR, Ringeman JL, et al. (2014) Angled dental implant placement into the vomer/nasal crest of atrophic maxillae for all-on-four immediate function: A 2-year clinical study of 100 consecutive patients.Int J Oral Maxillofac Implants, 29:e30-35. doi:10.11607/jomi.te39

60. Jung S, Lo LJ (2020) Dissection in the pyramidal space for effective relief of tension in cleft palate repair. Ann Plast Surg, 84:S54-S59. doi:10.1097/SAP.0000000000002169
61. Kang SH, Byun IY, Kim JH, et al. (2012) Three-dimensional analysis of maxillary anatomic landmarks for greater palatine nerve block anesthesia. J Craniofac Surg, 23:e199-202. doi:10.1097/SCS.0b013e31824de71b
62. Kizilkanat E, Boyan N, Ozsahin E, et al. (2011) Importance of craniofacial asymmetry in surgery. 21:147-149.
63. Klosek SK, Rungruang T (2009) Anatomical study of the greater palatine artery and related structures of the palatal vault: Considerations for palate as the subepithelial connective tissue graft donor site. Surg Radiol Anat, 31:245-250. doi:10.1007/s00276-008-0432-4
64. Kowalczyk KA, Majewski A (2021) Analysis of surgical errors associated with anatomical variations clinically relevant in general surgery. Review of the literature. Transl Res Anat, 23:100107.
65. Kraus BS, Decker JD (1960) The prenatal inter-relationships of the maxilla and premaxilla in the facial development of man. Acta Anat (Basel), 40:278-294. doi:10.1159/000141590
66. Langenegger JJ, Lownie JF, Cleaton-Jones PE (1983) The relationship of the greater palatine foramen to the molar teeth and pterygoid hamulus in human skulls. J Dent, 11:249-256. doi:10.1016/0300-5712(83)90197-5
67. Latham RA (1970) Maxillary development and growth: The septo-premaxillary ligament. J Anat, 107:471-478.
68. Latham RA (1971) The development, structure and growth pattern of the human mid-palatal suture. J Anat, 108:31-41.
69. Lee SP, Paik KS, Kim MK (2001) Variations of the prominences of the bony palate and their relationship to complete dentures in korean skulls. Clin Anat, 14:324-329. doi:10.1002/ca.1059
70. Liang X, Jacobs R, Martens W, et al. (2009) Macro- and micro-anatomical, histological and computed tomography scan characterization of the nasopalatine canal. J Clin Periodontol, 36:598-603. doi:10.1111/j.1600-051X.2009.01429.x
71. Marzook HAM, Elgendy AA, Darweesh FA (2021) New accessory palatine canals and foramina in cone-beam computed tomography. Folia Morphol (Warsz), 80:954-962. doi:10.5603/FM.a2020.0114
72. Matsuda Y (1927) Location of the dental foramina in human skulls from statistical observations Int J Orthod Oral Surg Radiogr, 13:299-305.
73. Methathrathip D, Apinhasmit W, Chompoopong S, et al. (2005) Anatomy of greater palatine foramen and canal and pterygopalatine fossa in Thais: Considerations for maxillary nerve block. Surg Radiol Anat, 27:511-516. doi:10.1007/s00276-005-0016-5
74. Mew J (1974) The incisive foramen--a possible point of reference. Br J Orthod, 1:143-146. doi:10.1179/bjo.1.4.143
75. Milanovic P, Selakovic D, Vasiljevic M, et al. (2021) Morphological characteristics of the nasopalatine canal and the relationship with the anterior maxillary bone-a cone beam computed tomography study. Diagnostics (Basel), 11doi:10.3390/diagnostics11050915
76. Mooney MP, Siegel MI (1986) Developmental relationship between premaxillary-maxillary suture patency and anterior nasal spine morphology. Cleft Palate J, 23:101-107.
77. Morand M, Irinakis T (2007) The challenge of implant therapy in the posterior maxilla: Providing a rationale for the use of short implants. J Oral Implantol, 33:257-266. doi:10.1563/1548-1336(2007)33[257:TCOITI]2.0.CO;2
78. Moreira RS, Sgrott EA, Stuker H, et al. (2008) Palatal asymmetry during development: An anatomical study. Clin Anat, 21:398-404. doi:10.1002/ca.20638

79. Mraiwa N, Jacobs R, Van Cleynenbreugel J, et al. (2004) The nasopalatine canal revisited using 2d and 3d ct imaging. Dentomaxillofac Radiol, 33:396-402. doi:10.1259/dmfr/53801969
80. Nasreddine G, El Hajj J, Ghassibe-Sabbagh M (2021) Orofacial clefts embryology, classification, epidemiology, and genetics. Mutat Res Rev Mutat Res, 787:108373. doi:10.1016/j.mrrev.2021.108373
81. Nasseh I, Aoun G, Sokhn S (2017) Assessment of the nasopalatine canal: An anatomical study. Acta Inform Med, 25:34-38. doi:10.5455/aim.2017.25.34-38.
82. Nicol P, Elmaleh-Berges M, Sadoine J, et al. (2020) Incidence and morphology of the incisive suture in ct scanning of young children and human fetuses. Surg Radiol Anat, 42:1057-1062. doi:10.1007/s00276-020-02521-8
83. Nimigean V, Nimigean VR, Butincu L, et al. (2013) Anatomical and clinical considerations regarding the greater palatine foramen. Rom J Morphol Embryol, 54:779-783.
84. O'Rahilly R, Gardner E (1972) The initial appearance of ossification in staged human embryos. Am J Anat, 134:291-301. doi:10.1002/aja.1001340303
85. Ortug A, Uzel MJFm (2019) Greater palatine foramen: Assessment with palatal index, shape, number and gender. 78:371-377.
86. Pan J, Tatum SA. rhinoplasty for cleft and hemangioma-related deformities. advanced aesthetic rhinoplasty: Springer; 2013:699-709.
87. Radlanski RJ, Emmerich S, Renz H (2004) Prenatal morphogenesis of the human incisive canal. Anat Embryol (Berl), 208:265-271. doi:10.1007/s00429-004-0389-y
88. Rapado-González O, Suárez-Quintanilla J, Otero-Cepeda X, et al. (2015) Morphometric study of the greater palatine canal: Cone-beam computed tomography. 37:1217-1224.
89. Rapado-Gonzalez O, Suarez-Quintanilla JA, Otero-Cepeda XL, et al. (2015) Morphometric study of the greater palatine canal: Cone-beam computed tomography. Surg Radiol Anat, 37:1217-1224. doi:10.1007/s00276-015-1511-y
90. Rossi M, Ribeiro E, Smith R (2003) Craniofacial asymmetry in development: An anatomical study. Angle Orthod, 73:381-385. doi:10.1043/0003-3219(2003)073<0381:CAIDAA>2.0.CO;2
91. Rude FP, Anderson L, Conley D, et al. (1994) Three-dimensional reconstructions of the primary palate region in normal human embryos. Anat Rec A Discov Mol Cell Evol Biol, 238:108-113. doi:10.1002/ar.1092380112
92. Rusu MC. Orofacial developmental anatomy. Bucharest: Ed.Infomedica; 2003.
93. Rusu MC. Oro-maxillofacial anatomy. Timișoara: Victor Babes Publishing House 2022.
94. Rusu MC, Sandulescu M, Carstocea L (2020) False and true accessory infraorbital foramina, and the infraorbital lamina cribriformis. Morphologie, 104:51-58. doi:10.1016/j.morpho.2019.12.003
95. Sadler TW. Langman's medical embryology: Lippincott Williams & Wilkins; 2011.
96. Santos PL, Silva GH, da Silva RD, et al. (2017) Implant anchorage in the nasopalatine canal for the rehabilitation of severely atrophic maxilla. Implant Dent, 26:324-327. doi:10.1097/ID.0000000000000562
97. Saralaya V, Nayak SR (2007) The relative position of the greater palatine foramen in dry Indian skulls. Singapore Med J, 48:1143-1146.
98. Sarnat BG. Postnatal growth of the nasomaxillary complex. Fundamentals of craniofacial growth: CRC Press; 2017:205-224.
99. Shahab S, Safavi M, Taleghani F, et al. (2021) Cbct evaluation of the position of palatal neurovascular bundle and the greater palatine foramen in an Iranian population. 33
100. Sheikhi M, Zamaninaser A, Jalalian F (2013) Length and anatomic routes of the greater palatine canal as observed by cone beam computed tomography. Dent Res J (Isfahan), 10:155-161. doi:10.4103/1735-3327.113324

101. Shelley A, Tinning J, Yates J, et al. (2019) Potential neurovascular damage as a result of dental implant placement in the anterior maxilla. Br Dent J, 226:657-661. doi:10.1038/s41415-019-0260-4
102. Sicher H (1962) Anatomy and oral pathology. Oral Surg Oral Med Oral Pathol, 15:1264-1269. doi:10.1016/0030-4220(62)90163-9
103. Sinha I, Poddar R, Basu R (2021) Morphometric analysis of hard palate in eastern Indian population.
104. Skrzat J, Holiat D, Walocha J (2003) A morphometrical study of the human palatine sutures Folia Morphol (Warsz), 62:123-127.
105. Song WC, Jo DI, Lee JY, et al. (2009) Microanatomy of the incisive canal using three-dimensional reconstruction of microct images: An ex vivo study. Oral Surg Oral Med Oral Pathol Oral Radiol Endod, 108:583-590. doi:10.1016/j.tripleo.2009.06.036
106. Soumya P, Koppolu P, Pathakota KR, et al. (2019) Maxillary incisive canal characteristics: A radiographic study using cone beam computerized tomography. Radiol Res Pract, 2019:6151253. doi:10.1155/2019/6151253
107. Starczewska M, Motyl S, Lipski M, et al. (2014) Premaxilla-development and significance in humans-systematic review of literature. J Stomatol, 67
108. Stipetic J, Hrala Z, Celebic A (2005) Thickness of masticatory mucosa in the human hard palate and tuberosity dependent on gender and body mass index. Coll Antropol, 29:243-247.
109. Stout FW, Collett WK (1969) Etiology and incidence of the median maxillary anterior alveolar cleft. Oral Surg Oral Med Oral Pathol, 28:66-72. doi:10.1016/0030-4220(69)90195-9
110. Studer SP, Allen EP, Rees TC, et al. (1997) The thickness of masticatory mucosa in the human hard palate and tuberosity as potential donor sites for ridge augmentation procedures. J Periodontol, 68:145-151. doi:10.1902/jop.1997.68.2.145
111. Suter VG, Jacobs R, Brucker MR, et al. (2016) Evaluation of a possible association between a history of dentoalveolar injury and the shape and size of the nasopalatine canal. Clin Oral Investig, 20:553-561. doi:10.1007/s00784-015-1548-7
112. Suzuki M, Omine Y, Shimoo Y, et al. (2016) Regional anatomical observation of morphology of greater palatine canal and surrounding structures.Bull Tokyo Dent Coll, 57:223-231. doi:10.2209/tdcpublication.2016-1100
113. Suzuki M, Omine Y, Shimoo Y, et al. (2016) Regional anatomical observation of morphology of greater palatine canal and surrounding structures. 57:223-231.
114. Sved AM, Wong JD, Donkor P, et al. (1992) Complications associated with maxillary nerve block anaesthesia via the greater palatine canal. Aust Dent J, 37:340-345. doi:10.1111/j.1834-7819.1992.tb00758.x
115. Tavassolizadeh H, Torkzadeh A, Kheiri L, et al. (2019) Evaluation of greater palatine canal and foramen anatomical variation on cone-beam ct radiography. 4:151-155.
116. Thakur AR, Burde K, Guttal K, et al. (2013) Anatomy and morphology of the nasopalatine canal using cone-beam computed tomography. Imaging Sci Dent, 43:273-281.
117. Thakur AR, Burde K, Guttal K, et al. (2013) Anatomy and morphology of the nasopalatine canal using cone-beam computed tomography. Imaging Sci Dent, 43:273-281. doi:10.5624/isd.2013.43.4.273
118. Tomaszewska IM, Kmiotek EK, Pena IZ, et al. (2015) Computed tomography morphometric analysis of the greater palatine canal: A study of 1,500 head ct scans and a systematic review of literature. Anat Sci Int, 90:287-297. doi:10.1007/s12565-014-0263-9
119. Tomaszewska IM, Tomaszewski KA, Kmiotek EK, et al. (2014) Anatomical landmarks for the localization of the greater palatine foramen--a study of 1200 head cts, 150 dry skulls, systematic review of literature and meta-analysis.J Anat, 225:419-435. doi:10.1111/joa.12221
120. Tozum TF, Guncu GN, Yildirim YD, et al. (2012) Evaluation of maxillary incisive canal characteristics related to dental implant treatment with computerized tomography: A clinical multicenter study. J Periodontol, 83:337-343. doi:10.1902/jop.2011.110326

121. Vasiljevic M, Milanovic P, Jovicic N, et al. (2021) Morphological and morphometric characteristics of anterior maxilla accessory canals and relationship with nasopalatine canal type-a cbct study. Diagnostics (Basel), 11doi:10.3390/diagnostics11081510
122. Viveka S, Kumar MJAP (2016) Radiological localization of greater palatine foramen using multiple anatomical landmarks. 2:187-189.
123. Von Arx T, Lozanoff S. Clinical oral anatomy: A comprehensive review for dental practitioners and researchers: Springer; 2016.
124. Von Arx T, Lozanoff S. Clinical oral anatomy: A comprehensive review for dental practitioners and researchers. Switzerland: Springer; 2016.
125. Wang TM, Kuo KJ, Shih C, et al. (1988) Assessment of the relative locations of the greater palatine foramen in adult Chinese skulls. Acta Anat (Basel), 132:182-186.
126. Warwick R, Williams P, Gray H. Gray's anatomy: Longman; 1973.
127. Westmoreland EE, Blanton PL (1982) An analysis of the variations in position of the greater palatine foramen in the adult human skull. Anat Rec A Discov Mol Cell Evol Biol, 204:383-388. doi:10.1002/ar.1092040412
128. Wu B, Li H, Fan Y, et al. (2020) Clinical and anatomical study of foramen locations in jaw bones and adjacent structures. Medicine (Baltimore), 99:e18069. doi:10.1097/MD.0000000000018069
129. Yilmaz HG, Boke F, Ayali A (2015) Cone-beam computed tomography evaluation of the soft tissue thickness and greater palatine foramen location in the palate. J Clin Periodontol, 42:458-461.
130. Yu SK, Lee MH, Park BS, et al. (2014) Topographical relationship of the greater palatine artery and the palatal spine. Significance for periodontal surgery. J Clin Periodontol, 41:908-913. doi:10.1111/jcpe.12288
131. Zivanovic S (1980) Longitudinal grooves and canals of the human hard palate. Anat Anz, 147:161-167.